

Spectral weight transfer and mass renormalization in Mott-Hubbard systems SrVO_3 and CaVO_3 : Influence of long-range Coulomb interaction

K. Morikawa, T. Mizokawa, K. Kobayashi, and A. Fujimori
Department of Physics, University of Tokyo, Bunkyo-ku, Tokyo 113, Japan

H. Eisaki and S. Uchida
Department of Applied Physics, University of Tokyo, Bunkyo-ku, Tokyo 113, Japan

F. Iga and Y. Nishihara
Electrotechnical Laboratory, Tsukuba, Ibaraki 305, Japan
 (Received 23 June 1995; revised manuscript received 21 July 1995)

We have studied metallic SrVO_3 and CaVO_3 by inverse photoemission and high-resolution photoemission. In going from Sr to Ca, considerable spectral weight is transferred from the coherent band to the upper and lower Hubbard bands. Meanwhile, the overall intensity rather than the width of the coherent band decreases, implying that the bandwidth remains finite as the system approaches the Mott transition. The result implies that the effect of long-range Coulomb interaction as well as short-range interaction becomes increasingly important towards the transition.

It is well known that electron correlation enhances the conduction electron mass m^* in metals. The mass should diverge toward a metal-insulator transition if the transition is of second order and the carrier number remains finite up to the transition point.¹ Recent studies of a filling-control system $\text{La}_{1-x}\text{Sr}_x\text{TiO}_3$ suggest that such a mass divergence indeed occurs in the electronic specific heats and the magnetic susceptibilities.^{2,3} In bandwidth-control systems, where the ratio between the interaction strength U and the bandwidth W is varied for a fixed band filling, a mass divergence has also been predicted by Brinkman and Rice.⁴ Recent studies of the infinite-dimension Hubbard model at half filling indicate that the coherent quasiparticle (QP) band, which crosses the Fermi level (E_F), is narrowed with U/W while the spectral intensity at E_F remains unaltered.⁵

In previous work,^{6,7} we made photoemission studies of various compounds with a d^1 configuration ranging from a Mott-Hubbard insulator to a normal metal (YTiO_3 , LaTiO_3 , SrVO_3 , VO_2 , and ReO_3) in order to investigate how the single-particle spectral function $\rho(\omega)$ evolves with U/W across the transition. The result has shown that, with increasing U/W , spectral weight is transferred from the coherent part (QP excitations) around E_F to the incoherent part (reminiscent of the lower Hubbard band) ~ 1.5 eV below E_F , but that the overall intensity rather than the bandwidth of the coherent part appears to decrease in contrast to what has been predicted by the Hubbard-model calculations. From analysis of the photoemission spectra using a phenomenological self-energy correction,⁷ it has been suggested that the mass enhancement associated with the spectral weight transfer is largely compensated for by the band widening which is represented by an increasing degree of the \mathbf{k} dependence of the self-energy. However, the limited energy resolution in the previous work^{6,7} has precluded detailed and unambiguous information about the low-energy electron-

ic structure of these compounds such as the presence or absence of the narrow QP band at E_F , as predicted theoretically.⁵

In order to clarify these points, we have performed detailed photoemission and inverse-photoemission spectroscopy [bremsstrahlung isochromat spectroscopy (BIS)] studies of two metallic compounds CaVO_3 and SrVO_3 . With much improved energy resolution, we have established that the intensity at E_F indeed decreases with U/W , and that there is no detectable narrow peak in the coherent part. We attribute the intensity decrease to the effect of nonlocal exchange potential arising from long-range Coulomb interaction, which limits the mass enhancement or band narrowing near the Mott transition.

SrVO_3 and CaVO_3 are both Pauli-paramagnetic metals.⁸⁻¹³ SrVO_3 has the cubic perovskite structure while CaVO_3 shows a tetragonal distortion of the GdFeO_3 type.⁸ Therefore the d -band-width $W \propto \cos^2\theta$, where θ is the V—O—V bond angle, is smaller by $\sim 15\%$ in CaVO_3 ($\theta \sim 155^\circ$ – 160°) than in SrVO_3 ($\theta \sim 180^\circ$). Single-crystalline CaVO_3 and SrVO_3 samples were prepared by the floating-zone method, and heated in air at about 170°C for several hours. Thermogravimetric analysis showed that the oxygen content of both samples were 3.03 ± 0.01 . Inductively coupled plasma atomic emission spectroscopy analysis showed that Ca-to-V ratio in CaVO_3 was stoichiometric to within experimental error of $\sim \pm 1\%$. Photoemission measurements were made at Synchrotron Radiation Laboratory, Institute for Solid State Physics, University of Tokyo. The energy resolution was ~ 0.35 eV at $h\nu \sim 60$ eV. High-resolution ($\Delta E \sim 35$ meV) photoemission measurements were performed on a spectrometer equipped with a helium discharge lamp ($h\nu = 21.2$ eV). BIS measurements were made using a SiO_2 multichromator ($h\nu = 1486.6$ eV), and the energy resolution was ~ 1 eV.

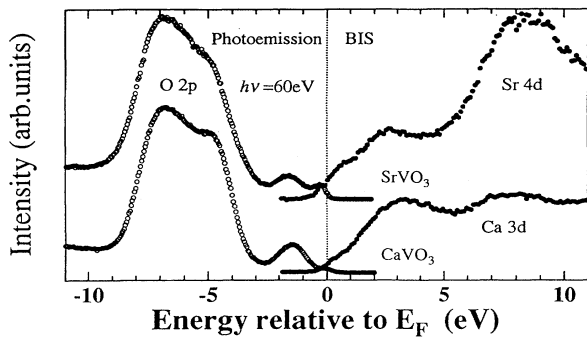


FIG. 1. Photoemission and BIS spectra taken at ~ 80 K.

The samples were cooled to liquid-nitrogen temperature or to ~ 30 K and were scraped *in situ* with a diamond file. Measurements were made within 15–30 min after scraping, in order to eliminate surface degradation.

Figure 1 shows combined photoemission and BIS spectra of SrVO_3 and CaVO_3 . Structures between -10 and -3 eV are due to the filled O $2p$ band and those around 8 eV are due to the empty Sr $4d$ or Ca $3d$ band, according to band-structure calculations performed using the local-density approximation (LDA).¹⁴ Structures between -3 and 5 eV are due to the partially filled V $3d$ band. As for the photoemission spectra, emission just below E_F well corresponds to the density of states (DOS) of the t_{2g} sub-band of V $3d$ as shown in Fig. 2, and is attributed to the

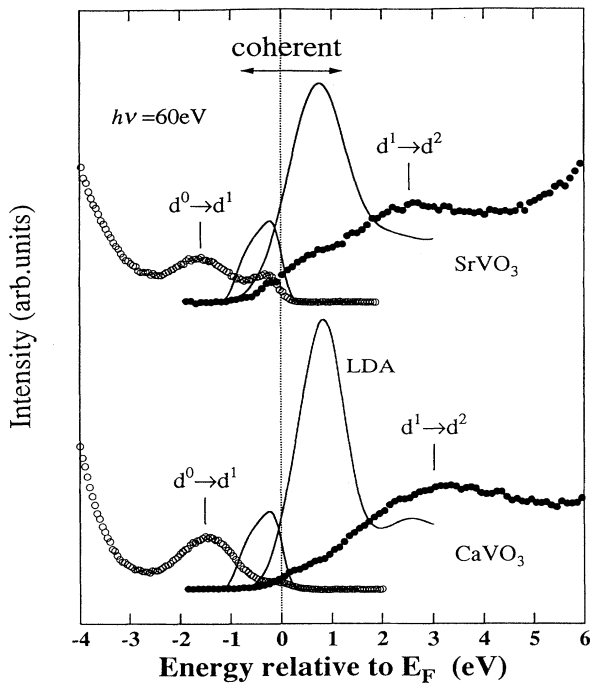


FIG. 2. Enlarged view of Fig. 1, compared with the DOS given by LDA band-structure calculations (Ref. 14) convoluted with a Gaussian representing the instrumental resolution (solid curves). The measured spectra and the calculated DOS have been normalized to the integrated area of the V $3d$ spectral weight.

coherent part of the V $3d$ spectral function.^{6,7} The peak at ≈ -1.6 eV has no corresponding feature in the band-structure calculations and is attributed to the incoherent part of the spectral function or a reminiscent of the lower Hubbard band.⁶ In the BIS spectra, the prominent peak at ~ 2.5 –3 eV and a shoulder at $\lesssim 1$ eV are assigned the incoherent and coherent parts of the spectral function, respectively, of the V $3d$ - t_{2g} origin in analogy with the photoemission spectra. Thus the BIS spectra are consistent with the picture that, with increasing U/W , the V $3d$ spectral weight is transferred from the coherent part to the incoherent part both below and above E_F . It can be noticed from Fig. 2 that the coherent band is somewhat (by a factor of ~ 1.5) narrower than the calculated d band.

The transport and magnetic properties of SrVO_3 and CaVO_3 do not change their character below ~ 300 K.^{8–15} Therefore, the high-resolution photoemission spectra near E_F shown in Figs. 3 and 4 indeed reflect low-energy excitations responsible for the thermodynamic properties of these compounds since the present energy resolution of ~ 35 meV corresponds to the temperature of ~ 140 K.¹⁵ Thus the spectra unambiguously indicate that the intensity at E_F decreases in going from SrVO_3 to CaVO_3 with increasing U/W . This is contrasted with the spectral function of the Hubbard model in infinite dimension,⁵ which shows a band narrowing rather than the intensity decrease.

Deviation of the spectral function from the local-density-approximation (LDA) band structure can be expressed as a self-energy correction $\Sigma(\mathbf{k}, \omega)$ to the LDA eigenvalues $\epsilon_{\mathbf{k}}$ as described in Ref. 7. The spectral intensity at E_F , $\rho(0)$, differs from that predicted by the LDA cal-

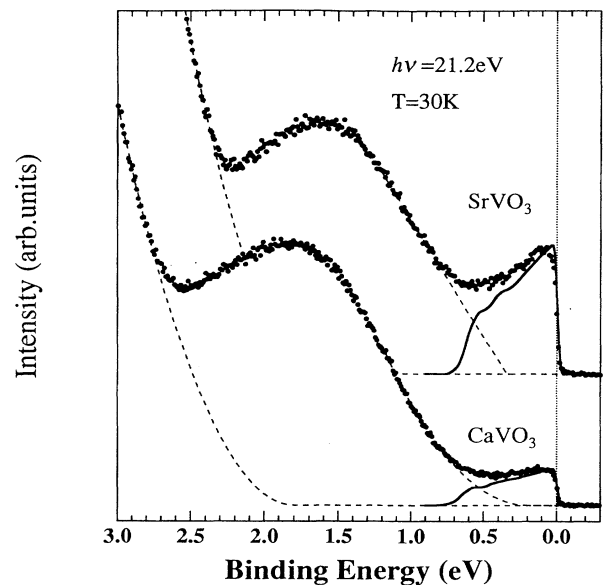


FIG. 3. High-resolution photoemission spectra taken at ~ 30 K. The broken curves show a decomposition of the spectra into the tail of the O $2p$ band and the incoherent and incoherent parts of the V $3d$ spectral weight. The solid curves are the DOS given by LDA band-structure calculations (Ref. 14) narrowed by a factor m_b/m^* .

ulation by the factor

$$\frac{m_k}{m_b} = \left| \frac{\partial \epsilon_k}{\partial \mathbf{k}} \right| \left/ \left| \frac{\partial \epsilon_k}{\partial \mathbf{k}} + \frac{\partial \text{Re}\Sigma(\mathbf{k}, \omega)}{\partial \mathbf{k}} \right| \right|_{\mathbf{k}=\mathbf{k}_F}, \quad (1)$$

where m_b is the bare band mass.¹⁶ m_k (referred to as the \mathbf{k} mass) differs from m_b when the self-energy is \mathbf{k} dependent. The QP mass m^* , which is inversely proportional to the coherent bandwidth and is equal to the thermal and transport masses, is given by $m^*/m_b = (m_\omega/m_b)(m_k/m_b)$,¹⁶ where m_ω is called the ω mass, defined by

$$\frac{m_\omega}{m_b} = 1 - \left. \frac{\partial \text{Re}\Sigma(\mathbf{k}, \omega)}{\partial \omega} \right|_{\omega=0}. \quad (2)$$

The ω dependence of the self-energy represents dynamical effects (electron correlation and/or electron-phonon interaction) and leads to a narrowing of the coherent band by the renormalization factor $z_k(\omega) \equiv [1 - \partial \text{Re}\Sigma(\mathbf{k}, \omega)/\partial \omega]^{-1}$ and to the appearance of the incoherent spectral weight away from E_F .⁷

If one assumes that $z_k(\omega)$ is constant ($\equiv m_b/m_\omega < 1$) throughout the coherent band, the coherent-to-incoherent spectral weight ratio is given by $m_b/m_\omega : (1 - m_b/m_\omega)$. From the remarkable spectral weight transfer from the coherent to the incoherent part in going from SrVO₃ to CaVO₃, it is likely that the spectral weight of the coherent part vanishes (i.e., $m_\omega \rightarrow \infty$), as the system approaches the Mott transition. The concomitant decrease of the spectral intensity at E_F implies that $m_k \rightarrow 0$ toward the Mott transition.

We have estimated the QP mass m^* from the coherent-to-incoherent spectral weight ratio [$= 1/(m_\omega/m_b - 1)$], and the spectral intensity at E_F ($\propto m_k/m_b$) using $m^* = m_\omega m_k/m_b$ as listed in Table I. In the previous photoemission study,⁷ a line-shape analysis was made for the coherent part using a model self-energy, giving a slightly larger m^*/m_b value of ~ 2.5 for CaVO₃. This is consistent with the present result considering the uncertainties due to the lower-energy resolution in the previous study and the ambiguity in separating the incoherent and coherent parts in both studies.

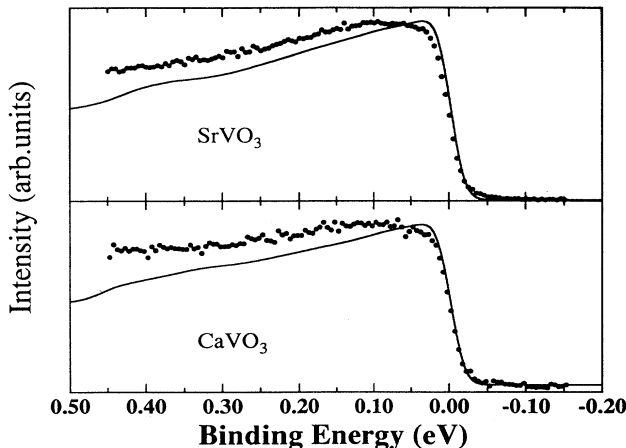


FIG. 4. The same as Fig. 3, but on an expanded scale.

Note that the QP masses of the two compounds are not appreciably different in spite of the conspicuous difference in the spectral weight transfer. Indeed, the optical spectra of both compounds^{17,9} yields nearly the same effective electron numbers ($\propto 1/m^*$) at about 1.5 eV. In Figs. 3 and 4, the calculated DOS has been narrowed by the factor m_b/m^* and is compared favorably with the coherent part of the measured spectra. The thermodynamic quantities, namely the electronic specific heats and the Pauli-paramagnetic susceptibilities given in Table I,^{8,10-13,17} show that the QP mass of CaVO₃ is at most $\sim 50\%$ larger than that of SrVO₃.¹⁸

The renormalization factor $z_k(\omega)$ becomes constant throughout the coherent part if $\Sigma(\mathbf{k}, \omega)$ can be decomposed into a \mathbf{k} -dependent part and an ω -dependent part: $\Sigma(\mathbf{k}, \omega) = \Sigma(\omega) + \Sigma(\mathbf{k})$, where $\text{Re}\Sigma(\omega) = -a\omega$ and $\Sigma(\mathbf{k}) = \alpha\epsilon_k$.^{7,19} While there is no rigorous microscopic justification for this, a separation of $\Sigma(\mathbf{k}, \omega)$ into $\Sigma(\omega)$ and $\Sigma(\mathbf{k})$ has been proposed in a simplified form of the so-called GW approximation.²⁰ The screened Coulomb interaction $W(\mathbf{r}-\mathbf{r}', t)$ which appears in the GW calculations can be decomposed into an effective short-range interaction W_{SR} and the remaining long-range interaction W_{LR} as $W(\mathbf{r}-\mathbf{r}', t) = W_{\text{SR}}(\mathbf{r}-\mathbf{r}', t) + W_{\text{LR}}(\mathbf{r}-\mathbf{r}', t)$.²¹ The short-range interaction largely contributes to the local $\Sigma(\omega)$, while the long-range interaction contributes a plasmon-pole structure around the plasma frequency to $\Sigma(\omega)$ (Ref. 22) and a nearly ω -independent nonlocal potential to $\Sigma(\mathbf{k})$. The long-range potential is generally screened in metals. However, since the screening length cannot be smaller than the average electron-electron distance, the long-range Coulomb interaction is not well screened at least between nearest-neighbor V atoms. In the LDA, the nonlocal exchange potential arising from the long-range interaction has been replaced by a local potential and therefore should include $\Sigma(\mathbf{k})$ in the present analysis.

If m^* does not diverge but approaches a constant value toward the Mott transition, $m_\omega \rightarrow \infty$ and $m_k \rightarrow 0$ mean that both $\partial \Sigma(\omega)/\partial \omega|_{\omega=\epsilon_F}$ and $\partial \Sigma(\mathbf{k})/\partial \mathbf{k}|_{\mathbf{k}=\mathbf{k}_F}$ are equally divergent toward the transition [see Eqs. (1) and (2)]. While the divergent behavior of $\partial \Sigma(\omega)/\partial \omega|_{\omega=\epsilon_F}$ has been expected,^{1,4} $\partial \Sigma(\mathbf{k})/\partial \mathbf{k}|_{\mathbf{k}=\mathbf{k}_F}$ may also diverge because the long-range Coulomb interaction would be less efficiently screened near the transition. [Note that in the Hartree-Fock approximation, $\partial \Sigma(\mathbf{k})/\partial \mathbf{k}$ shows a logarithmic divergence on the Fermi surface for the unscreened long-range Coulomb interaction.] According to the Hartree-Fock approximation, the nonlocal exchange

TABLE I. ω mass (m_ω), \mathbf{k} mass (m_k), and QP mass (m^*) in SrVO₃ and CaVO₃.

	m_ω/m_b	m_k/m_b	m^*/m_b	
			photoemission	thermodynamic
SrVO ₃	6.0 ± 0.6	0.24 ± 0.03	1.4 ± 0.3	$3.7^a, 3.6^b, 2.4^c, 4.2^d$
CaVO ₃	20 ± 2	0.068 ± 0.007	1.3 ± 0.3	$5.6^a, 4.7^c, 3.7^d$

^aReference 8.

^dReference 13.

^bReference 17.

^cReference 12.

^eReference 11.

potential contributes a dispersion width of order $\sim e^2/\epsilon d$, where ϵ is the optical dielectric constant and d is the average electron-electron distance (which is equal to the cubic lattice parameter of the perovskite lattice in the present case). If this contribution remains finite up to the transition, the coherent bandwidth ($\propto 1/m^*$) cannot be smaller than $\sim e^2/\epsilon d$, no matter how strong the band narrowing due to $\Sigma(\omega)$ becomes, that is, no matter how strongly m_ω diverges. It then follows that $m_k \rightarrow 0$ as $m_\omega \rightarrow \infty$, since $m_k = m^* m_b / m_\omega$. For typical values of $d \sim 4$ Å and $\epsilon \sim 3-5$, we find $e^2/\epsilon d \sim 0.5-1$ eV, which explains the observed width of the coherent part.

The m^*/m_b values deduced from the thermodynamic measurements are 2–3 times larger than those deduced here (Table I). This indicates that the band narrowing is not entirely uniform throughout the coherent band but is somewhat stronger near E_F . In Fig. 4, one notices an intensity decrease from ≈ 0.1 eV toward E_F , which is not predicted by the LDA calculations plus the uniform band narrowing and is therefore due to a change in $\Sigma(\mathbf{k})$ near E_F . This feature might be related to the existence of the low-energy scale responsible for the thermodynamic mass enhancement.

For electrons interacting through long-range Coulomb interaction, only those electrons with energies lower than the average electron-electron repulsion ($|\omega| < e^2/\epsilon d$) will repel each other. This will explain why the suppression of the spectral intensity occurs within the coherent band of width $\sim e^2/\epsilon d$. It is interesting to note that a similar energy scale $\sim e^2/\epsilon d$ appears in quasi-one-dimensional

systems of electrons interacting through long-range Coulomb interaction.²³ Here d represents the average electron-electron distance along the chain. For $|\omega| < e^2/\epsilon d$, the spectral function is strongly suppressed compared to the noninteracting band DOS and exhibits a power-law dependence $\rho(\omega) \propto |\omega|^\alpha$ characteristic of a Tomonaga-Luttinger liquid.

In conclusion, comparison between the photoemission spectra of SrVO₃ and CaVO₃ has revealed no compelling evidence of a divergence of the QP mass toward the Mott transition. The moderate mass enhancement compared to the strong spectral weight transfer is explained as due to the nonlocal exchange contribution from the long-range Coulomb interaction, which limits the narrowing of the overall coherent bandwidth as the system approaches the transition. Unfortunately, one cannot reach a Mott transition in the Sr_{1-x}Ca_xVO₃ system. Studies of such a system, where one can vary U/W continuously across the transition, are strongly desired. Spectroscopic studies on filling-control systems, in which m^* apparently diverges,² are also of great interest to see how m_k and m_ω behave as the system approaches the Mott transition.

We thank A. Sekiyama, K. Mamiya, and the staff of the Synchrotron Radiation Laboratory for technical support, and I. H. Inoue and M. J. Rozenberg for useful discussions. This work is supported by a Grant-in-Aid for Scientific Research from the Ministry of Education, Science and Culture of Japan and by the New Energy and Industrial Technology Development Organization.

¹M. Imada, J. Phys. Soc. Jpn. **63**, 3059 (1994).

²Y. Tokura, Y. Taguchi, Y. Okada, Y. Fujishima, T. Arima, K. Kumagai, and Y. Iye, Phys. Rev. Lett. **70**, 2126 (1993).

³Y. Fujishima, Y. Tokura, T. Arima, and S. Uchida, Phys. Rev. B **46**, 11 167 (1992).

⁴W. F. Brinkman and T. M. Rice, Phys. Rev. B **2**, 4302 (1970).

⁵X. Y. Zhang, M. J. Rozenberg, and G. Kotliar, Phys. Rev. Lett. **70**, 1666 (1993).

⁶A. Fujimori, I. Hase, H. Namatame, Y. Fujishima, Y. Tokura, H. Eisaki, S. Uchida, K. Takegahara, and F. M. F. de Groot, Phys. Rev. Lett. **69**, 1796 (1992).

⁷I. H. Inoue, I. Hase, Y. Aiura, A. Fujimori, Y. Haryuama, T. Maruyama, and Y. Nishihara, Phys. Rev. Lett. **74**, 2539 (1995).

⁸B. L. Chamberland and P. S. Danielson, J. Solid State Chem. **3**, 243 (1971).

⁹M. Kasuya, Y. Tokura, T. Arima, H. Eisaki, and S. Uchida, Phys. Rev. B **47**, 6193 (1993).

¹⁰K. Kumagai, K. Kawano, T. Suzuki, H. Takahashi, M. Kasuya, Y. Fujishima, Y. Yamaguchi, and Y. Tokura, Physica B **186-188**, 1030 (1993); (unpublished).

¹¹M. Onoda, H. Ohta, and H. Nagasawa, Solid State Commun. **79**, 281 (1991).

¹²A. Fukushima, F. Iga, I. H. Inoue, K. Murata, and Y.

Nishihara, J. Phys. Soc. Jpn. **63**, 409 (1994).

¹³H. Eisaki, Ph.D. thesis, University of Tokyo, 1991.

¹⁴K. Takegahara, J. Electron Spectrosc. Relat. Phenom. **66**, 30 (1994). The DOS at E_F is calculated to be 1.6 states/eV/formula unit.

¹⁵The temperature broadening of the Fermi-Dirac distribution function is $\sim 4kT$.

¹⁶C. W. Greef, H. R. Glyde, and B. E. Clements, Phys. Rev. B **45**, 7951 (1992).

¹⁷P. Dougier, J. C. C. Fan, and J. B. Goodenough, J. Solid State Chem. **14**, 247 (1975).

¹⁸In deducing the m^*/m_b values listed in Table I, the Stoner factor (~ 1.8) (Refs. 10 and 13) was assumed to be the same for SrVO₃ and CaVO₃.

¹⁹In Ref. 7, it has been assumed that $\Sigma(\omega) = g\gamma\Delta\omega/(\omega+i\gamma)(\omega+i\Delta)$.

²⁰L. Hedin, Phys. Rev. **139**, A796 (1965).

²¹F. Gygi and A. Baldereschi, Phys. Rev. Lett. **62**, 2160 (1989).

²²Dynamical effects included in the present $\Sigma(\omega)$ may not be solely due to electron correlation as discussed in Refs. 20 and 21, but could also be due to electron-phonon interaction.

²³A. Sekiyama, A. Fujimori, S. Aonuma, H. Sawa, and R. Kato, Phys. Rev. B **51**, 13 899 (1995).